

Fundamental Properties of Shrinkage Cracking of High Performance Fiber Reinforced Cement-Based Composites

K. Kirikoshi and H. Mihashi
Tohoku University, Sendai, Japan

ABSTRACT: High Performance Fiber Reinforced Cement-based Composites (HPFRCC) are provided with high ductility with multiple cracking, thin crack width and pseudo-strain hardening behavior. Such mechanical properties are expected to serve for a long service life of concrete structures. However, HPFRCC usually have high cement content per unit volume but no coarse aggregates. Therefore they have a high risk of shrinkage induced cracking. In this paper, some results of experimental study on drying shrinkage of HPFRCC are presented. Restrained shrinkage tests with three different geometries and four mix proportions including plain mortar were carried out. Besides the influence of the specimen's geometry, the influence of specimen's size and degree of restraint was studied.

1 INTRODUCTION

For the sake of preserving global environment and the sustainability, it is expected for buildings and infrastructures to have a long service life. Many concrete structures, however, suffer from durability problems and the service life is sometimes not sufficiently long. Many of these problems are initiated by cracking in the cover concrete of reinforced concrete members. The most possible source of the crack initiation is shrinkage of concrete.

High Performance Fiber Reinforced Cement-based Composites (HPFRCC) have been developed and recently they started to be widely used in practice. The most characteristic properties of HPFRCC are of its high ductility provided with multiple cracking, thin crack width and pseudo-strain hardening behavior. Therefore recently HPFRCC is often called Strain Hardening Cement-based Composites (SHCC). While HPFRCC can be highly resistant to cracking, usually they have a high value of cement content per unit volume of the matrix and they usually don't contain any coarse aggregates. As a result, they have a high risk of shrinkage cracking, though the crack can be much thinner than that in normal concrete. Thus, for designing rationally the materials of HPFRCC, it is very important to quantify the capability of resistance against shrinkage cracking and to understand well the efficiency of fiber reinforcement in the materials under the condition subjected to restrained shrinkage. For that purpose, standard test methods are essential

though any test methods suitable for this very ductile material have not been standardized, yet.

Several test methods have been developed to assess the cracking resistance of concrete and they are reviewed in several literatures (e.g. Grysbowski et al. 1990 & Weiss et al. 1998). In the meantime, the American Association of State Highway and Transportation Officials (AASHTO) developed a provisional standard in 1989 that recommends a ring test with 300mm inner diameter, 75 mm thickness and 150 mm height of concrete wall, and 12 mm thickness of steel wall. For measuring the shrinkage stress acting on the ring specimen, the standard uses strain gages which are placed at mid-height on the inner circumference of the steel ring. Because of the simplicity, the ring test has been commonly used over the last two decades to assess the risk of shrinkage cracking in concrete (Akhter & Weiss 2004). While there have been a limited number of papers published on shrinkage induced cracking in HPFRCC, most of them were carried out by means of the ring tests, too. However, various sizes and thickness of steel ring and HPFRCC specimens were adopted.

Wittmann et al. (2002) studied the risk for crack formation in HPFRCC under shrinkage by means of a ring test. A sensitivity analysis of the material properties was carried out to find the possibility to optimize the composition of the cement-based materials with respect to the crack formation. Weimann and Li (2003) carried out an experimental study of Engineered Cementitious Composites (ECC) that is a kind of HPFRCC containing PVA fiber of 2 vol.%

and they showed that an average crack width was 31 and 46 micrometer depending on the shrinkage of the matrix.

In this paper, a series of experimental study on HPFRCC is carried out by means of different test methods for surveying which test method is most suitable to study the evolution of shrinkage stress and crack formation in HPFRCC as the first step to set up a standard test method for determining the capability of resistance against shrinkage cracking. For this purpose, four material compositions including plain mortar and three types of passive restraining techniques for shrinkage were applied. Besides the influence of specimen's geometry, the influence of specimen's size and degree of restraint was studied.

2 EXPERIMENTAL PROGRAM

2.1 Materials and mixture proportions

The mortar matrix was made with early strength Portland cement, silica sand whose diameter was about 0.09 mm, silica fume and a viscous agent. PVA fiber (REC-15, Kuraray) of two different length (6 mm and 12 mm) was used. The mix proportion of the tested materials is shown in Table 1. Besides the mortar used as the matrix of HPFRCC (i.e. PLAIN series), three types of HPFRCC were tested. Among them, PVA-12-1 and PVA-12-2 series contain 1 vol.% and 2 vol.% of PVA fiber of 12 mm, respectively. PVA-6-2 contains 2 vol.% of PVA fiber of 6 mm. After mixing all the components in a pan-type mixer of 50 liters capacity, the fresh mortar with or without fibers was placed in molds and compacted. Then they were covered with a plastic film to prevent moisture loss and maintained in a room of 20 °C and RH=60% for 7 days. Specimens were demolded at the age of 7 days.

Table 1. Composition of tested materials (kg/m³).

Material Series	Water (kg/m ³)	Cement (kg/m ³)	Silica fume (kg/m ³)	Silica sand (kg/m ³)	Viscous agent (kg/m ³)	PVA fiber		
						weight (kg/m ³)	length (mm)	content (vol.%)
PLAIN	554	715	179	357	7.76	0	–	–
PVA-6-2	543	701	175	350	7.60	26	6	2
PVA-12-1	549	708	177	354	7.68	13	12	1
PVA-12-2	543	701	175	350	7.60	26	12	2

2.2 Material properties

At the age of 7 days, compressive strength and elastic modulus were measured by cylinder tests. Tension tests were also carried out on dumbbell type specimens of 13mm thickness and of 30mm width to determine the tensile material properties such as crack initiation stress, the maximum tensile stress and the corresponding strain. The results of tension tests are shown in Fig.1. Table 2 shows fundamen-

tal material properties. All of them are mean values obtained from three specimens concerned.

Table 2. Material properties.

Material Series	Comp. strength f_c (MPa)	Elastic modulus E (GPa)	Crack initiation stress (MPa)	Maximum Tensile Stress (Mpa)	Tensile strain at the Max Stress ($\times 10^{-6}$)	Density (g/cc)
PLAIN	17.4	7.37	1.98*	1.98*	–	1.60
PVA-6-2	16.7	7.18	1.72	2.47	18025	1.57
PVA-12-1	20.4	7.20	1.34	2.26	22075	1.63
PVA-12-2	16.1	7.76	1.62	3.45	56179	1.59

* This value was obtained with splitting tests on cylindrical specimens.

Table 3. Geometry of specimens and tested number.

Geometry Series	Size of specimens (mm)	Tested material series and number of specimens			
		PLAIN	PVA-6-2	PVA-12-1	PVA-12-2
JIS type	–	/	2	/	/
Linear restrained type	100 × 100 × 1500	2	2	2	2
	50 × 50 × 750 (restraining rebar D16)	2	2	2	2
Restraining ring type	Thickness of steel ring t=10	/	2	/	/
	t=15	/	2	/	/
	t=30	/	2	/	/
Free shrinkage type	50 × 50 × 200	0	2	0	0
	100 × 100 × 400	2	2	2	2
	80 × 80 × 140	0	2	0	0

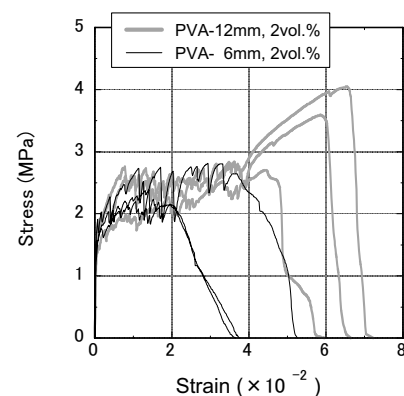
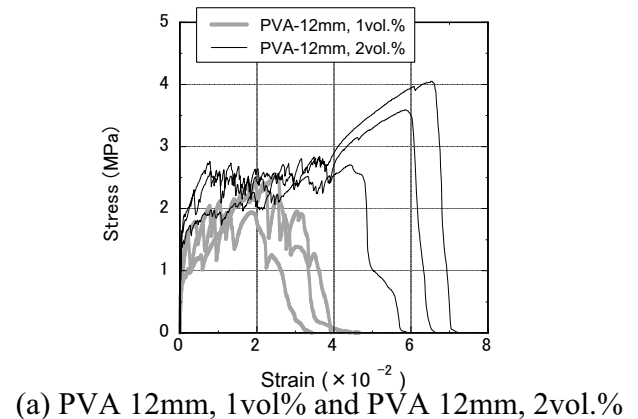


Figure 1. Stress-strain relationship obtained from dumbbell type tension tests.

2.3 Specimen geometry and measurement for drying shrinkage

Several different geometries of specimens were prepared for shrinkage measurement as shown in Fig. 2. Table 3 shows the tested number. The strain measurement started at the age of 1 day. Because of the rather high water-binder (W/B) ratio, autogenous shrinkage was negligible and it was confirmed by the shrinkage measurement. Drying shrinkage started at the age of 7 days in the laboratory atmosphere with RH=60% at 20 ° C.

Fig. 2(a) shows a kind of cracking frame test method which restrains the shrinkage by the external steel frame. This is a Japanese standard to measure the crack resistance of concrete (JIS A 1151). Shape of section in the central part of the tapered specimen was 100x100 mm. The restraining stress to cause cracking in concrete was measured with strain gages glued on the channel steel columns. In this study, a mold strain gage (PMFL-50-2LT, Tokyo Sokki Kenkyujo) was used to measure directly the shrinkage strain of the central part of the specimen, too.

Fig.2(b) shows a test method using linear type specimen which contains a deformed bar of D32 at the center of the section of 100x100 mm. The total length of the deformed bar was 1500 mm and the central part of the deformed bar was rounded for 300 mm to be $\phi 31$ mm, the bond of which was eliminated by three layers of a bondless plastic sheet. As a result, concrete specimen at the central part can shrink freely but the deformation is restrained at both sides with bond stress of the deformed bar. This test method has been recommended for autogenous shrinkage by JCI (1996). Fig. 2(c) shows a test method, the geometry of which is the same as that of JCI recommendation shown in Fig. 2(b) but the difference was only the size. All of the dimension is the half of the JCI recommendation. The degree of restraint by the steel bar was the same but crack initiation may occur in a much shorter age because of the higher rate of drying than that of the longer one. It is most easy for handling the test among methods shown in Fig.2.

Fig. 2(d) shows a ring test used in this study, the geometry of which is 380 mm outer diameter, 40 mm wall thickness, and 140 mm height. As for the thickness of the steel wall, three different values of 10, 15 and 26 mm were adopted. This variable is to investigate the influence of the degree of restraint that may cause a different cracking behavior.

Finally Fig. 2(e) shows prism specimens of $100 \times 100 \times 400 \text{mm}^3$, $50 \times 50 \times 200 \text{mm}^3$ and $80 \times 80 \times 140 \text{mm}^3$ for free shrinkage and water loss tests as a function of drying time. Four surfaces ($100 \times 400 \text{mm}^2$ or $50 \times 200 \text{mm}^2$) of the first two prisms were opened. These are comparative to series L and S of the linear type specimens, respec-

tively. On the other hand, however, only two sides of the surfaces ($80 \times 140 \text{mm}^2$) were opened in case of the last prisms which are comparative to the specimens of ring test since the wall thickness of the ring specimen was 40mm.

The shrinkage strain was measured with a mold gage every 10 minutes at the center of the specimen and the water loss was measured every 24 hours. Results of the strain gage were used as a reference value to determine the degree of restraint for shrinkage.

Shrinkage induced stress in HPFRCC of linear type specimens and JIS type specimens were determined by the following equations.

<Linear type specimens>:

$$\sigma(t) = \varepsilon_s(t) A_s E_s / (A - A_s) \quad (1)$$

<JIS type specimens>:

$$\sigma(t) = \varepsilon_s(t) A_s E_s / A_c \quad (2)$$

where

$\sigma(t)$: shrinkage induced stress at the drying time t(day)

$\varepsilon_s(t)$: compressive strain of restraining steel at the drying time t(day)

A: total section area of linear type specimen

A_s : section area of restraining steel

A_c : section area of HPFRCC specimen.

On the other hand, the maximum stress of ring test at the interface between the HPFRCC and steel ring was determined by equations theoretically obtained for a cylindrical shell with thick wall based on an elastic continuum mechanics (Tsuboi 1968). According to the theoretical equation, tangential stress: $\sigma_\theta(r)$ in the wall at a point r distant from the center O of cylindrical thick shell under uniform internal and external pressure is given by Eq.(3) and Eq. (4) (Fig. 3 (a)).

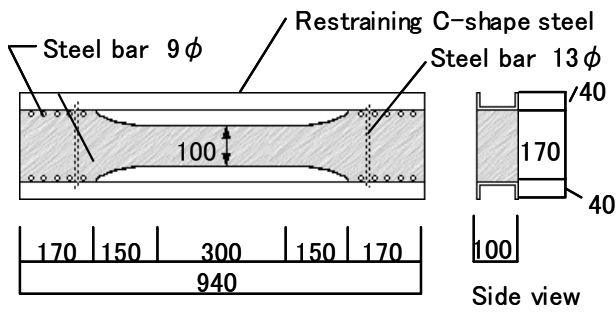
<in case under only internal pressure>: ($p_o = 0$)

$$\sigma_\theta(r) = p_i r_i^2 (r^2 + r_o^2) / r^2 (r_o^2 - r_i^2) \quad (3)$$

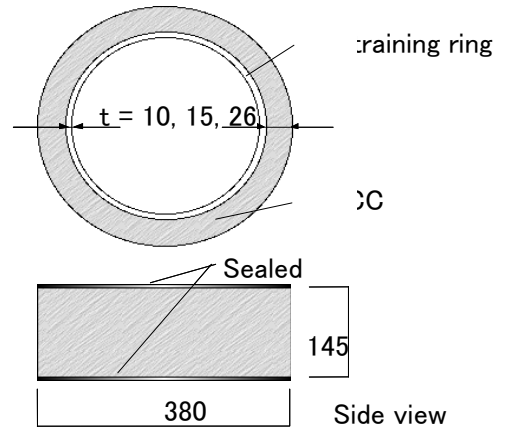
< in case under only external pressure>: ($p_i = 0$)

$$\sigma_\theta(r) = p_o r_o^2 (r^2 + r_i^2) / r^2 (r_o^2 - r_i^2) \quad (4)$$

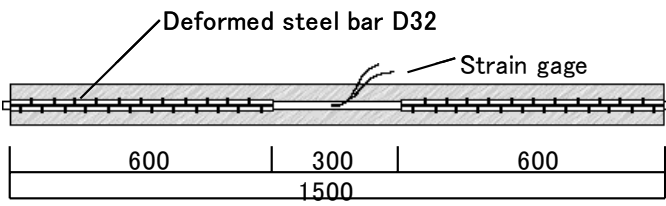
Equation (4) gives the stress on the internal surface of steel ring under the unknown pressure acting externally on the steel ring. Since this stress should be the same as that measured with strain gage on the internal surface of the steel ring, the unknown pressure can be determined. Then the determined pressure can be applied on the HPFRCC ring as the internal pressure, and Eq. (3) gives the maximum stress at the interface between the HPFRCC and steel ring (Fig. 3 (b)).



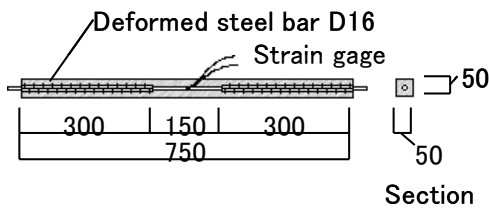
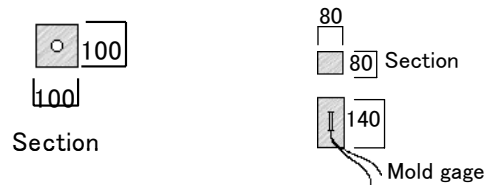
(a) JIS type



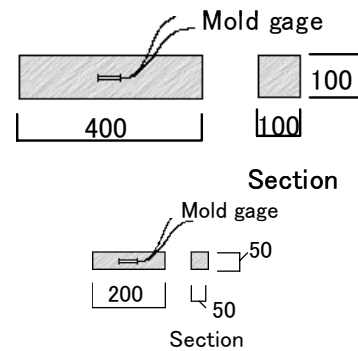
(d) Ring type restrained with a steel ring



(b) Long linear type restrained with a steel bar (L-series)

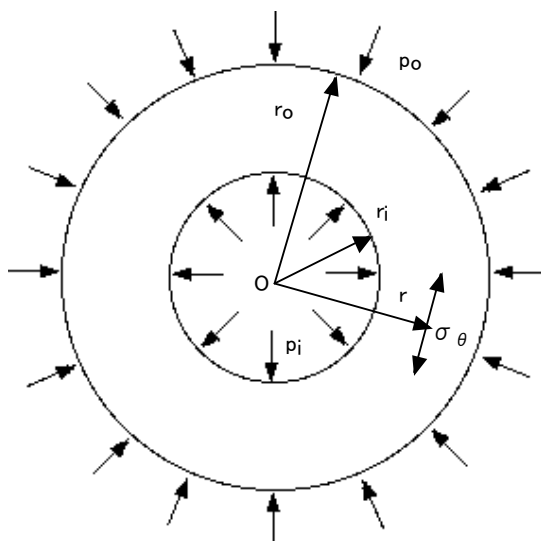


(c) Short linear type restrained with a steel bar (S-series)

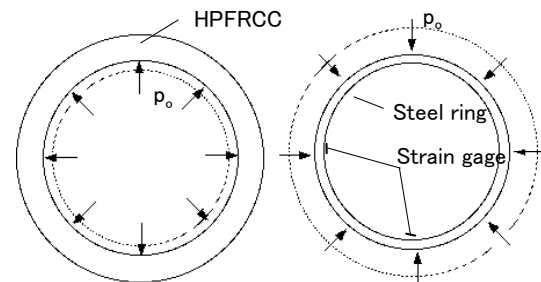


(e) Free shrinkage type

Figure 2. Geometry of drying shrinkage test specimens.



(a) Uniformly pressured thick cylindrical shell



(b) Equilibrium condition for the pressure

Figure 3. Schematic description of geometry and equilibrium condition for ring test.

Degree of restraint for the drying shrinkage in each test method was determined by Eq. (5).

$$\text{Degree of restraint} = \frac{\text{(free shrinkage - restrained shrinkage)}}{\text{(free shrinkage)}} \quad (5)$$

Crack widths at the center of linear type specimens restrained with a steel bar and all of the main cracks in ring type specimens were measured every two or three days with a crack gage. In the linear specimens, shrinkage cracking occurred in the part of both sides gripped with the deformed bar before the cracking occurred at the center, though the crack width at the center became the maximum soon after the initiation.

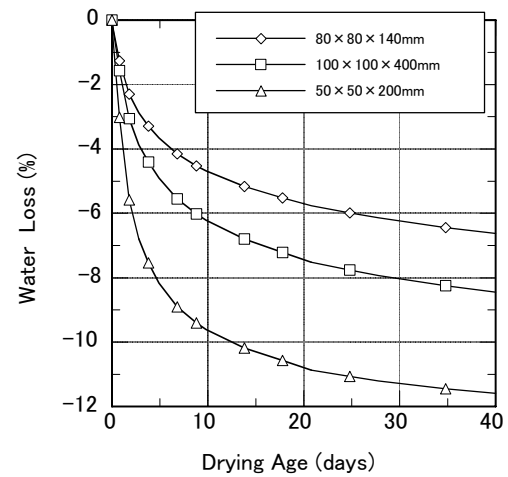
3 EXPERIMENTAL RESULTS AND DISCUSSION

3.1 Water loss and free drying shrinkage

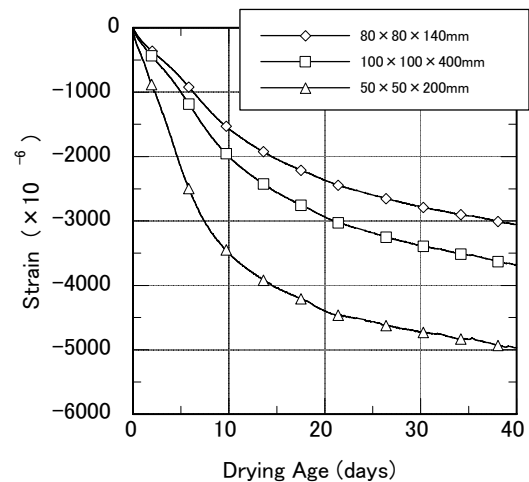
Figure 4 shows experimental results of water loss and free drying shrinkage as a function of drying age. These results were obtained from the prism specimens shown in Fig. 3(e). The rate of water loss is clearly influenced by the different volume vs. surface ratio (V/S) and the slope of the descending curve is very steep especially during the first 7 days. On the other hand, the curvature of the drying shrinkage during the first 7 days is obviously different from that of the water loss though the macroscopic tendency is similar to that of water loss. That might be due to the influence of moisture gradient created in the section of specimens during the first couple of days and it may mean that drying from the surface is so fast but not much reflected on the shrinkage strain in the central part of the specimen.

3.2 Shrinkage stress development

Figure 5 shows the development of shrinkage induced tensile stress in HPFRCC specimens as a function of drying age. It is clearly shown by the results of linear type specimens in Fig. 5 that the size of the specimen and the ductility of the material have a strong influence on the evolution of shrinkage stress and crack formation. Especially in case of shorter specimens (S-series), evolution of shrinkage stress is much more significant than that of longer specimens (L-series), though the difference between S and L in case of PVA-12-2 became smaller than the other case. The rapid evolution of shrinkage stress can be related to the rate of water loss shown in Fig.4. However, the crack initiation stress determined by the uniaxial tension test shown in Table 2 could not be directly related to these results as the crack initiation criteria.



(a) Water loss



(b) Free shrinkage strain

Figure 4. Water loss and free shrinkage as a function of drying age.

In most cases of S-series, the stress rapidly increased and then suddenly decreased for a moment. In cases of L-series, however, the increasing rate of the stress development is rather low and the rate became much lower at about the same age of the sudden decrease in case of S-series. These difference between S-series and L-series might be caused by different moisture gradient, crack initiation and distribution of cohesive stress bridging the crack i.e. ductility. Even after the sudden decrease, a certain level of the shrinkage stress still remained and the ductility of the material has influence on the stress level. Although HPFRCC of sufficiently high ductility such as PVA-12-2 series may not be influenced on the results, the smaller specimen may have a risk to give unsafe results for assessing the crack resistance due to shrinkage because S-series gave a higher shrinkage stress. More than 14 days measurement are required to obtain a stable stress condition in these linear type shrinkage tests.

Unique parameter focused in the ring test was the influence of degree of restraint. The thickness of the inner steel ring was varied for 10mm, 15mm and

26mm. As a result, a noticeable result was obtained. Up to about 1.3 MPa of the shrinkage stress at the interface of HPFRCC ring, the stress evolution was almost same. While of course the strain measured by strain gages on the inner surface of the steel ring was quite different among these three specimens, the theoretical treatment given by Eq. (3) and Eq. (4) gave the very clear solution. In other words, only because of that treatment, the influence of ductility on the shrinkage cracking behavior in the ring test was clearly shown. Stress evolution in both cases of thinner steel ring (10mm and 15mm) increased up to about 2.5 MPa. After the peak stress, shrinkage stress decreased and finally much lower values of about 1.8-2.0 MPa were obtained. On the other hand, in case of thicker steel ring of 26mm, a

shrinkage crack initiated at about 1.3 MPa and suddenly decreased for a moment. Then stress gradually increased again up to about 1.5 MPa and the stress level was remained. This might be due to the bridging of fibers across the crack, though the stress level was much lower than that of the maximum stress shown in Table 2.

The shrinkage evolution in case of JIS type specimens was very different from other cases. The maximum value of shrinkage induced stress was about 1 MPa. The main difference between JIS type test and other two types of test is the restraining position for the specimen which has similar moisture gradient in the section. Relaxation effect on cracking in HPFRCC could be less in case of JIS type in comparison with other two types.

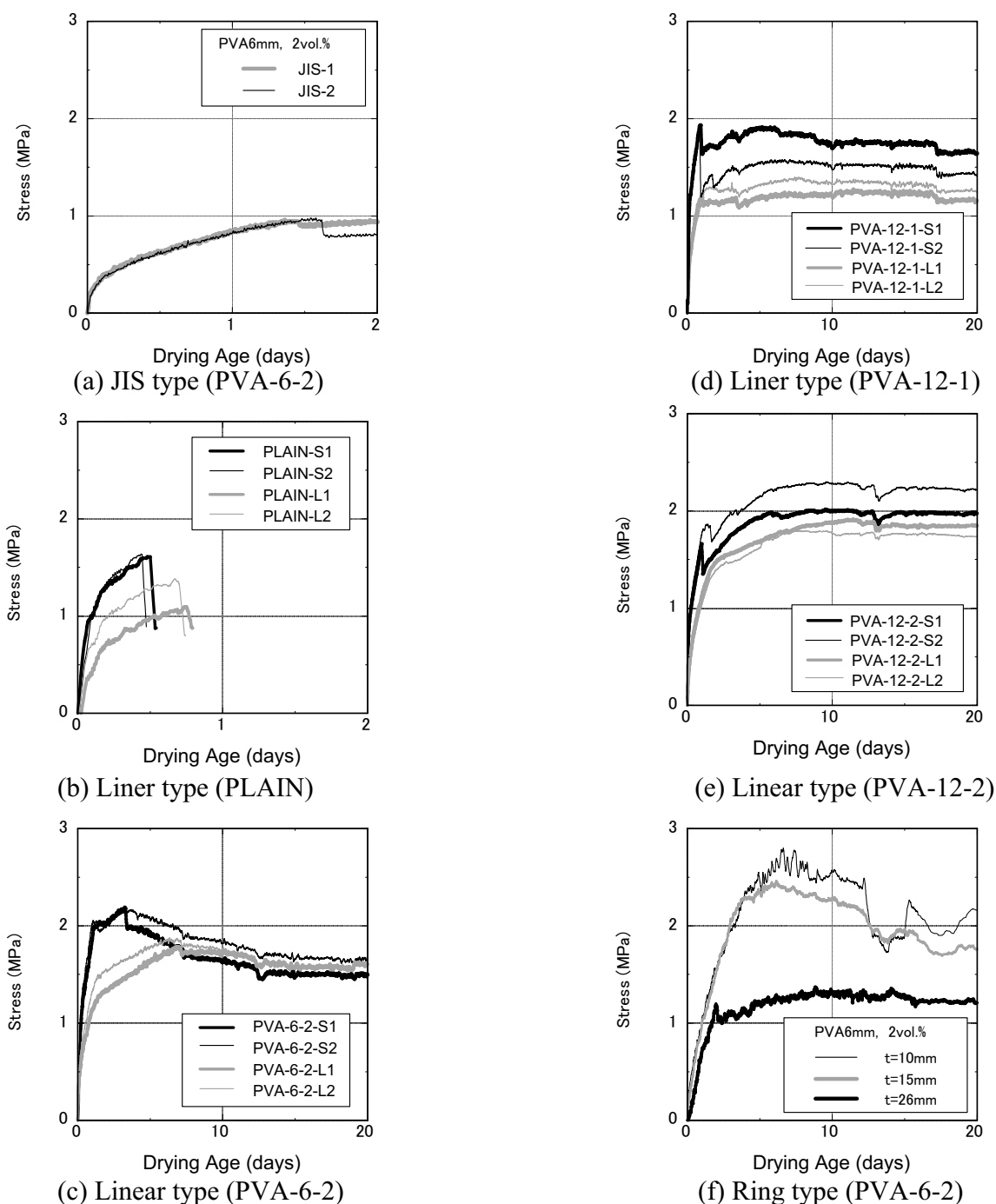


Figure 5. Shrinkage induced stress in HPFRCC specimens of various geometries.

3.3 Degree of restraint

Fig. 6 shows the influence of specimen's geometry on the degree of restraint as a function of drying age. Material series used for this comparative study was only PVA-6-2. In cases of linear type specimens and JIS type specimens, it is clearly shown that the restraint rate of S-series is higher than that of L-series. The noticeable point is that in cases of the linear type specimens and ring type specimens the restraint rate gradually increased and approached to a certain final value. On the other hand, the value in case of JIS type specimens showed an almost constant value or approached to a constant value from an early age.

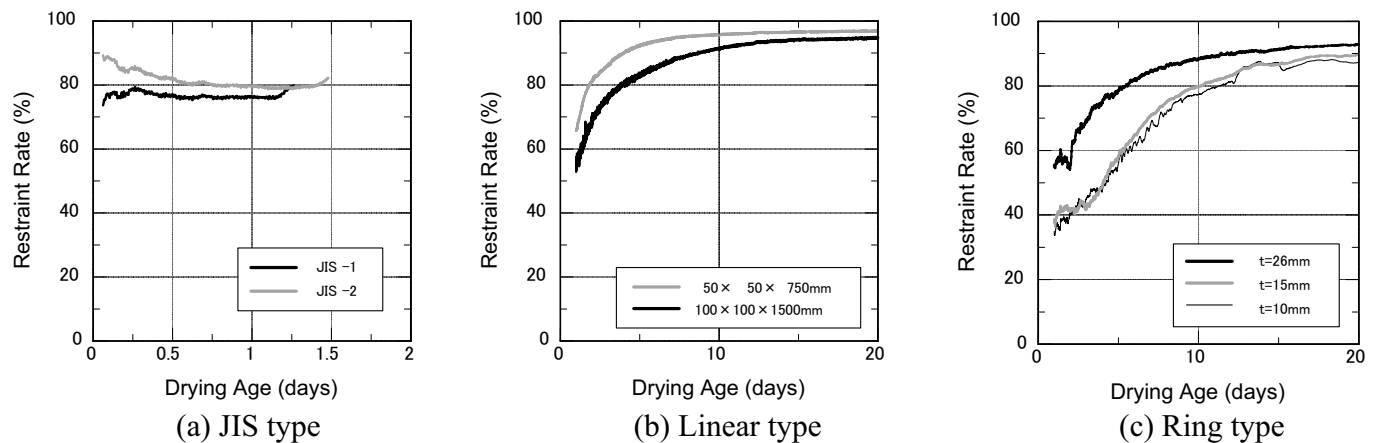


Figure 6. Degree of restraint for each test with PVA-6-2 series.

3.4 Evolution of crack width

Figure 7 shows the evolution of crack width as a function of drying age. Fig. 7(a) shows the influence of materials and specimen's size which were observed in linear type specimens. Crack width in plain mortar of larger specimens increased more significantly than that in smaller specimens. On the other hand, HPFRCC showed much less influence of size of the specimens and the crack width was much thinner than those of plain mortar as expected. In Fig. 7(b), evolution processes of main crack on the ring specimens are shown. The largest crack increased closing to 1mm at 30 days but most of others were kept within a much thinner ranges. These results may prove that the bridging mechanism across a crack by fibers working in HPFRCC has a great potential to prevent the opening of cracks on the surface of concrete structures but some other additional consideration against shrinkage induced cracking may be necessary for practical application where cracking in concrete is really critical. For that purpose, some chemical agents and arranging some grooves for inducing shrinkage cracking may work well to avoid cracking in other parts.

Influence of restraint degree was clearly observed in case of the ring test specimen with the thickest steel ring (26mm) but the other two cases (10mm and 15mm) didn't show any clear difference. The thicker the steel ring, handling of the shrinkage test becomes more difficult. However, from the mechanical view point, ring tests with a high degree of restraint may give a useful information about the crack resistance against shrinkage induced cracking such as creep and/or relaxation effects on bridging of fibers across the cracks.

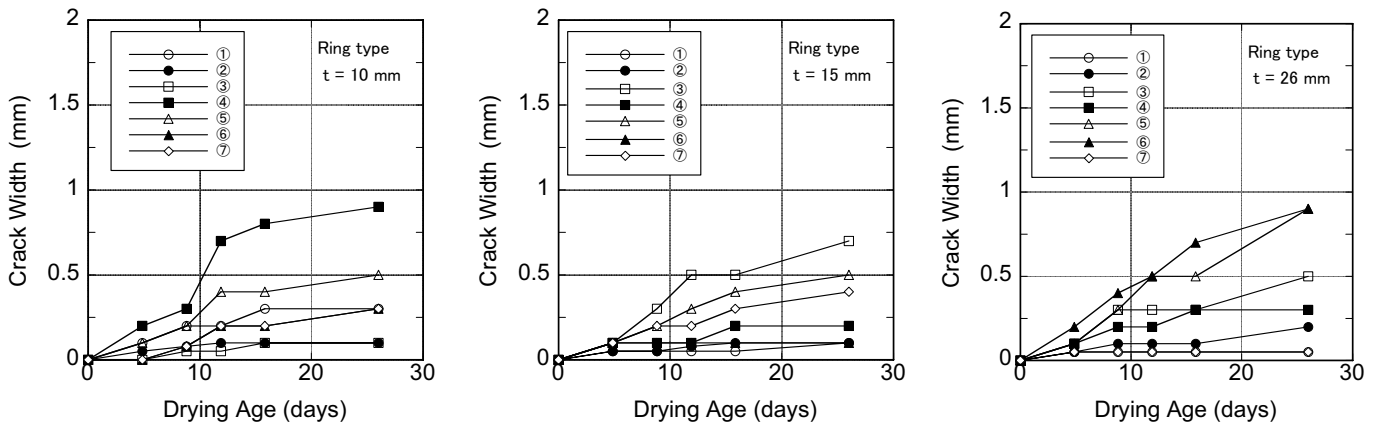
4 CONCLUDING REMARKS

Influence of specimen's geometry and degree of restraint on shrinkage induced cracking and stress evolutions were experimentally studied. The following conclusions were obtained.

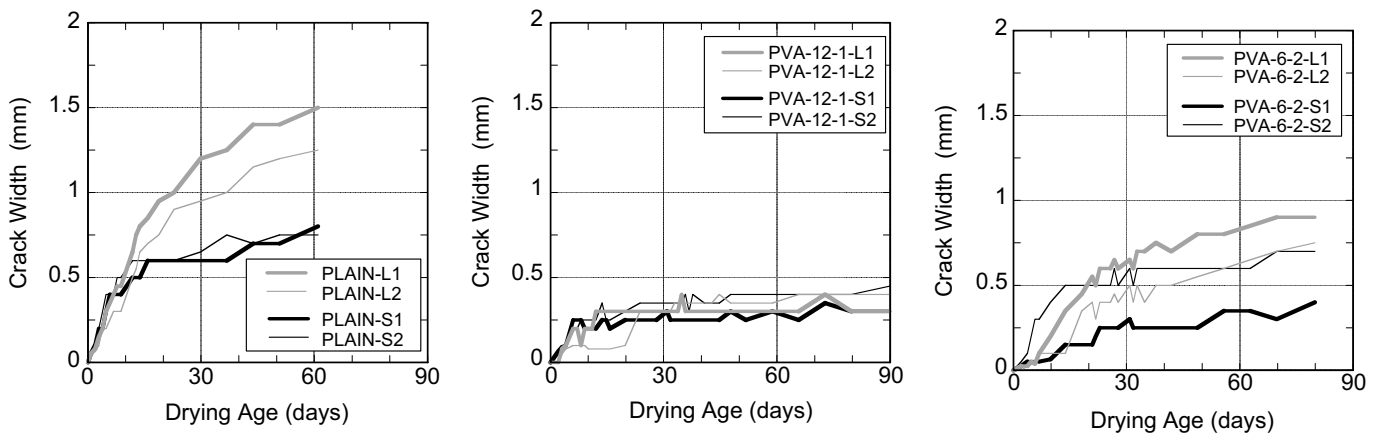
1. Crack initiation stress due to shrinkage is not directly related to the tensile strength obtained by static uniaxial tension tests.
2. Scale effects on stress evolution are significant and specimens of smaller section showed higher values of shrinkage stress.
3. Crack initiation stress is not proportional to the degree of restraint. A certain value of high degree is necessary to assess the crack resistance of HPFRCC by means of passive restraining techniques for shrinkage unless the restraint degree is comparative to that of the targeted structural member.

ACKNOWLEDGEMENT

The authors gratefully acknowledge the supports received from the Japan Cement Association under a grant offered in 2006.



(b) Restraining ring type specimens: Influence of restraint rates.



(a) Liner restrained type specimens: Influence of materials and specimen's size.

Figure 7. Evolution of crack width as a function of drying age.

REFERENCES

- AASHTO, (1989). Standard practice for estimating the crack tendency of concrete. *AASHTO Designation*, PP-34-89, 179-182.
- Grysbowski, M. and Shah, S.P. (1990). Shrinkage cracking of fiber reinforced concrete. *ACI Mater. J.* 87 (2), 138-48.
- Hossain, A.B. and Weiss, J. (2004). Assessing residual stress development and stress relaxation in restrained concrete ring specimens. *Cement & Concrete Composites*, 26, 531-540.
- JCI (1996). Committee report on autogenous shrinkage of concrete. 199-201 (in Japanese).
- Shah, H.R. and Weiss, J. (2006). Quantifying shrinkage crack in fiber reinforced concrete using the ring test. *Materials and Structures*, 39, 887-899.
- Tsuboi, Y. (1968). Elasto-plasticity in Building Structure, Shokokusha, 55-57. (in Japanese).
- Weimann, M.B. and Li, V.C. (2003). Hygral behavior of engineered cementitious composites (ECC). *Int. J. Restoration* 9, 513-534.
- Weiss, W.J., Yang, W. and Shah, S.P. (1998). Shrinkage cracking of restrained concrete slabs. *ASCE Journal of Engineering Mechanics* 124 (7), 765-74.
- Wittmann, F.H., Martinola, G. and Sadouki, H. (2002). Material properties influencing early cracking of concrete. *Control of Cracking in Early Age Concrete*, Mihashi & Wittmann (eds.) Swets & Zeitlinger, Lisse, 3-18.